

An experimental-numerical study on the vibro-acoustic characterization of honeycomb lightweight panels

M. Vivolo¹, B. Pluymers, D. Vandepitte, W. Desmet

¹ K.U.Leuven, Department Mechanical Engineering,
Celestijnenlaan 300 B, B-3001, Heverlee, Belgium
email: marianna.vivolo@mech.kuleuven.be

Abstract

Lightweight components are widely used in several technology sectors such as in transport and machine design and an appropriate knowledge about their vibro-acoustic performance characteristics is desired already in early design stages. Although they are able to offer a highly attractive weight saving, lightweight structures often exhibit unsatisfactory dynamic, i.e. noise and vibration, reduction skills. Among different indices commonly used within the research field, in this work the focus is on the acoustic Insertion Loss (IL) evaluation to describe the vibro-acoustic behaviour of lightweight panels. A simple test set-up is developed and used in order to experimentally investigate the transmission properties of different panels. Furthermore, several numerical studies allow the construction of an updated numerical model which can be used to predict the vibro-acoustic characteristics of lightweight structures mounted in the test set-up.

1 Introduction

To enhance vehicle performance and efficiency a designer nowadays looks more and more at the application of lightweight material components and takes advantage of the appealing weight saving offered by these kind of structures improving the final product and making it more competitive. Apart from transport, lightweight structures find their way into other engineering fields as well (aerospace, building construction, machine design and more). In the application of lightweight structures, care must be taken with respect to the vibro-acoustic characteristics and noise reduction capabilities. Due to their low mass, often also the dynamic and static stiffness are degraded which yields unsatisfactory vibro-acoustic performance and which in the end can ruin the global NVH (Noise, Vibration & Harshness) targets of the final product or vehicle. Often additional damping material is then added in a final troubleshooting campaign phase, resulting in a substantial reduction of the expected weight gain. Good a-priori knowledge of the vibro-acoustic properties of the applied lightweight structures is of crucial importance.

Fortunately, a structure built up of lightweight materials has a high number of configuration parameters which can be used to improve its functional performance. A lot of studies have already been carried out to understand, enhance and manipulate both the structural [1-3] and acoustic [4-6] properties of these complex structures. Great effort is also made to establish the sensitivity with respect to material and/or geometrical uncertainties and variability, inherently present in the structure [7] or sometimes intentionally introduced [8].

This paper continues the work reported in [9-10] and discusses an efficient tool to predict some of the transmission properties of lightweight panels, both experimentally and numerically. The experimental test set-up, located in a semi-anechoic room, consists of a (quasi-)rigid acoustic cavity that is closed by the panel under investigation. The excitation is provided by a loudspeaker situated on the bottom part of the

cavity. Insertion Loss (IL) evaluations based on radiated power measurements are collected using an intensity probe. The numerical model consists of a detailed structural Finite Element (FE) model of the studied plate, coupled to an acoustic indirect boundary element model of the acoustic cavity. The model is updated in order to get a satisfactory agreement with the experimental results, regardless of the specific examined panel. Two examples are shown: the case of a homogenous aluminium plate and of a more sophisticated TorHex honeycomb panel [11-13], both used to validate the optimised model.

The specimen with a fixed size (directly related to the set-up dimensions) and panel with Boundary Conditions (BCs) that can be modelled with precision (clamped boundary conditions are difficult to implement in reality) represent the two main restraints of this work. One could also include in this list of limitations the use of the IL index itself when looking at the vibro-acoustic properties in general. Indeed, particular attention must be paid looking at the results in terms of IL. It is defined as the difference in dB between the acoustic power radiated without enclosing component (“open cavity”) and the power radiated when a specimen is mounted on the top of the cavity (“closed cavity”) [14]

$$IL = 10 \log \frac{P_{without_panel}}{P_{with_panel}} \quad (1)$$

Thus, on the one hand the experimental procedure is not very demanding, as only two measurements of the sound power are necessary to determine the IL, and in general it is applicable also for complex structures. On the other hand, however, the IL also depends on the considered enclosure and its acoustics. It is a property of a specific pair of structure and cavity coupled to each other and not a characteristic of the panel alone. Unlike the IL, the Transmission Loss (TL) is another index that gives information about the acoustic transmission performance of the structural panel alone [15]

$$TL = 10 \log \frac{P_{Incident_ (source_room)}}{P_{Transmitted_ (receiving_room)}} \quad (2)$$

However, its experimental evaluation requires a specific and expensive acoustic test set-up which consists of 2 rooms. (i) A source room, that can be either reverberant (if one aims to get the structural response to a random incident field) in which a diffuse acoustic field has to be generated and the incident power has to be recorded (avoiding direct field effects and cavity resonances), or which can be anechoic (if one is interested in the response to a specific inclination of the incident field). (ii) A receiving anechoic room that approximates the free-field conditions. A rigid separating wall is located in between the two rooms, containing the specimen but not coupling the two cavities together.

In view of the complexity of TL measurements and the required test set-up, in this paper the IL approach is chosen to investigate the test panels. As such, during the interpretation of the results, the acoustic behaviour of the cavity needs to be taken into account.

This paper is structured in four sections. A description of the experimental set-up is given in the first part together with some details of the tested specimens (one TorHex core sandwich panel and one aluminium plate). The second section deals with the developed numerical model, partially updated on the basis of previous Experimental Modal Analyses (EMA) carried out on the examined panels. The final updated model is presented in the third section, followed by a comparison with the experimental results and final conclusions, given in the last part.

2 Experimental set-up

2.1 Acoustic cavity

The test set-up situated in a semi-anechoic room, consists of a box representing a (quasi-)rigid acoustic cavity, with a built-in loudspeaker on the bottom part. A schematic view is shown in Figure 1. Although the cavity is designed to be rigid, validation of simulations with measurements indicates that the walls

have some finite impedance. This will be further discussed in section 4. Till then, the cavity is considered to be perfectly rigid.

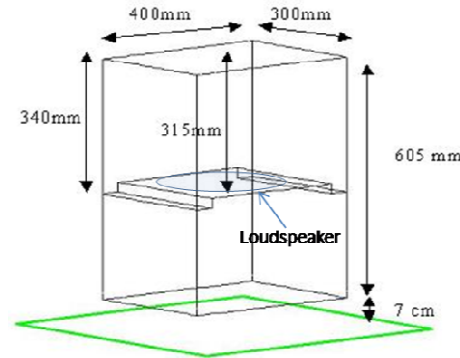


Figure 1: Schematic view of the box

The box actually comprises two acoustic cavities. The upper part has a size of 400mm x 300mm, while the height is 315mm for the most. The lower cavity has no other purpose than hosting the loudspeaker coil. In order to realise a rigid wall structure, the 50mm thick vertical walls of this box consist of two wooden panels filled with sand. Figure 2 shows some pictures of the test set-up.

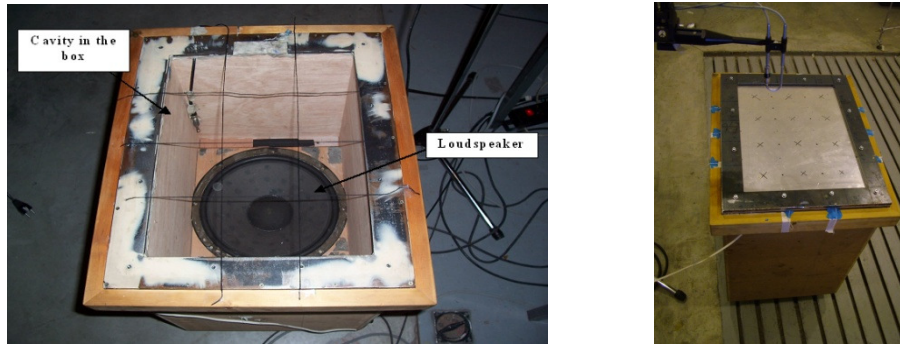


Figure 2: Open box on the left – Enclosed cavity on the right

This “sand-box” is placed in a semi-anechoic room, designed to absorb sound waves above 300Hz. This means that standing waves may occur below this threshold. The radiated power is calculated from intensity measurements, recorded by scanning the top surface of this set-up with an intensity probe (B&K type 3584) above the specimen (Figure 2 right side). The acquisition grid contains 12 measurement points, corresponding to the centre points of the 12 sub-surfaces (10cm x 10cm) in which the projection of the specimen surface on the measurement plane is decomposed (in Figure 2 left side, this corresponds to the black wire-net placed on the top of the cavity; in the picture on the right, to the black crosses marked on the plate). The space between the two ¼ inch microphones of the intensity probe is 50mm, making the measurements reliable in the frequency range [20-1250] Hz (intensity probe-spacer application limit). A random signal is provided to the loudspeaker in the frequency band [0-2560] Hz. LMS.TestLab Rev.8b is used to record and analyse the intensity values.

2.2 Specimen characteristics

The dimensions of a horizontal section of the described sand-box allows only specimen panels with a width w in the range of 300mm to 400mm and length l in the range of 400mm to 500mm. Any plate which satisfies these geometrical conditions can be tested, always with a wetted area of 400mm x 300mm

(because of the inner cavity size). As already mentioned, this represents a physical limit of this set-up. In order to validate the optimised numerical model developed for the experimental sand-box, two different panels are tested. One is a homogeneous aluminium plate, while the other one is a more complex structure, which consists of a sandwich panel with skin of polypropylene reinforced with natural fibres and TorHex paper core. A short description of these two systems follows in the next two paragraphs.

2.2.1 Homogeneous aluminium panel

A homogeneous aluminium plate with dimensions listed in Table 1 is experimentally investigated in order to build up and verify the updated numerical model.

Geometrical features	
Length	450mm
Width	350mm
Thickness	3mm

Table 1: Homogeneous aluminium panel geometrical properties

Figure 2 (right side) shows the assembly of the experimental set-up when this panel is clamped on the top of the acoustic cavity. The clamped BCs are realised by mounting a steel frame (5kg) on the top of the aluminium panel and connecting it to the wooden walls with 12 bolts (with 12 matching holes in the aluminium plate). The radiated acoustic power is measured by scanning with the intensity probe in a plane above the panel. Different distances are considered in the range from 5cm to 25cm. The effect on the resulting IL is negligible. The experimental and numerical acoustic power and IL shown in the remainder of this paper are evaluated in a plane at 25cm above the top of the cavity. The acquisition grid contains 12 measurement points. For the aluminium panel the test surface is also scanned once over a higher number of points (35) in order to better visualise the intensity distribution for some frequencies as will be shown later on. The frequency resolution is 1Hz. Each measurement consists of 21 averages and is carried out three times (63 averages per sub-surface central point).

2.2.2 TorHex core honeycomb panel

The vibro-acoustic behaviour of a sandwich panel with TorHex paper core and skin of polypropylene reinforced with natural fibres is investigated. Characteristic dimensions are given in Tables 2 and 3 in the global and detailed scales respectively. Table 3 also shows the material properties [16-17]. Figure 3 shows a picture of the TorHex core and a schematic view of this sandwich structure.

Global geometrical features	
Length	496mm
Width	387mm
Thickness	5mm

Table 2: TorHex sandwich panel global geometrical properties

Unit cell scale geometrical features					
Component	E_{MD} [GPa]	E_{CD} [GPa]	ρ [kg/m ³]	ν [-]	Thickness [mm]
Skin	2	2	451	0.2	0.55
Reinforced wall (core)	5	2	636	0.2	0.25
Cellular wall (core)	4.76	1.6	636	0.2	0.1

Table 3: TorHex sandwich panel detailed geometrical and material properties
(MD = manufacturing direction, CD = cross-wise direction)

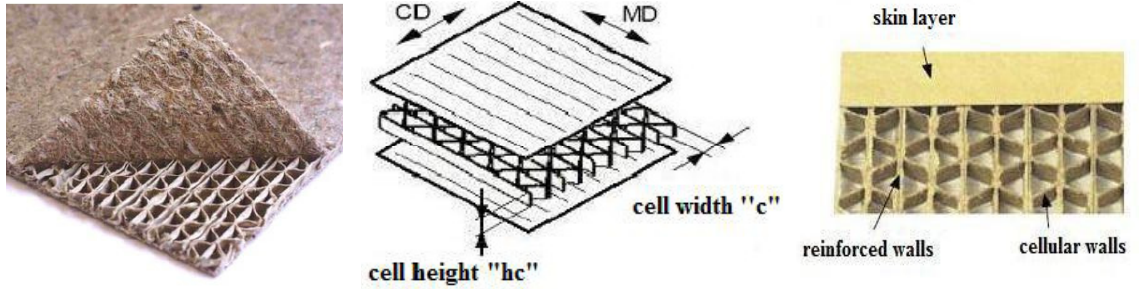


Figure 3: Detail of the TorHex paper core on the left – Schematic view of this panel on the right

A picture of the final assembly of the experimental set-up with the described panel mounted on the sand-box is reported in Figure 4.

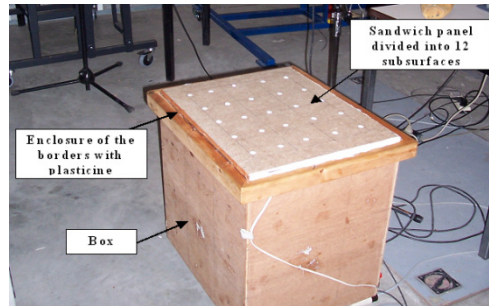


Figure 4: TorHex core sandwich panel with polypropylene skin mounted on the top of the sand-box

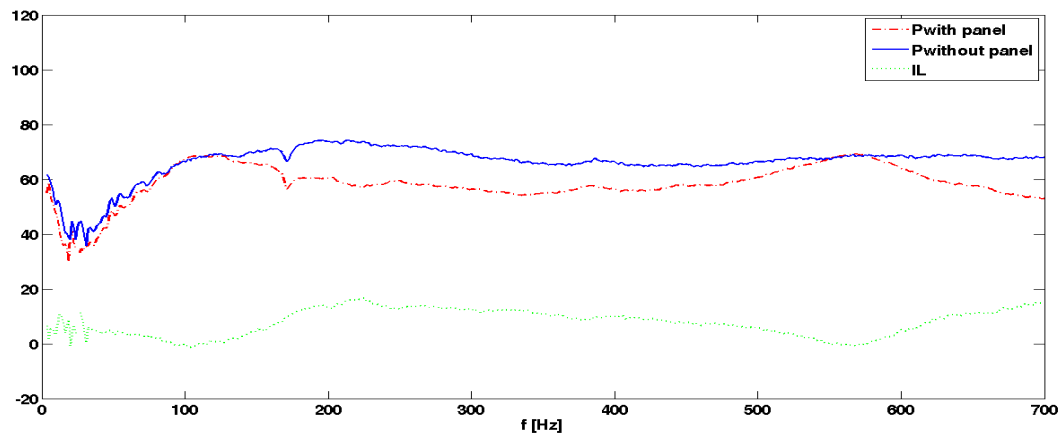
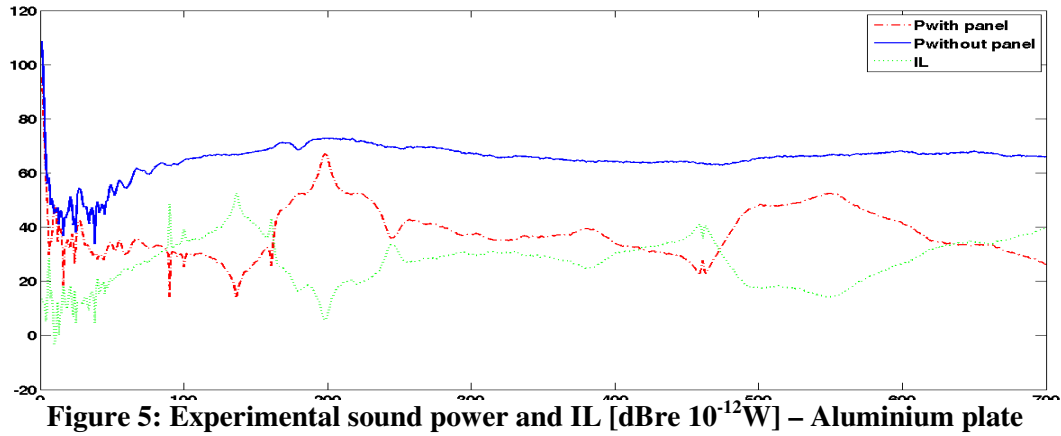
When mounted on this box the TorHex panel is simply supported (clamping could damage the core material). Since it is not a perfectly flat surface, plasticine is used to seal the edges. Therefore, an unknown amount of damping is added to the system and the BCs are not unambiguously known. This makes the numerical modelling not trivial and requires an iterative updating procedure as will be remarked also later on. The acoustic intensity is collected in 12 points in a plane at 5cm above the specimen (as mentioned this distance does not influence the IL evaluation, as far as kept the same for both the acquisitions for the open and closed cavity cases). The frequency resolution is 1.25Hz (0.8sec observation time). Each measurement consists of 15 averages and is carried out three times (45 averages per sub-surface central point).

2.3 Experimental IL

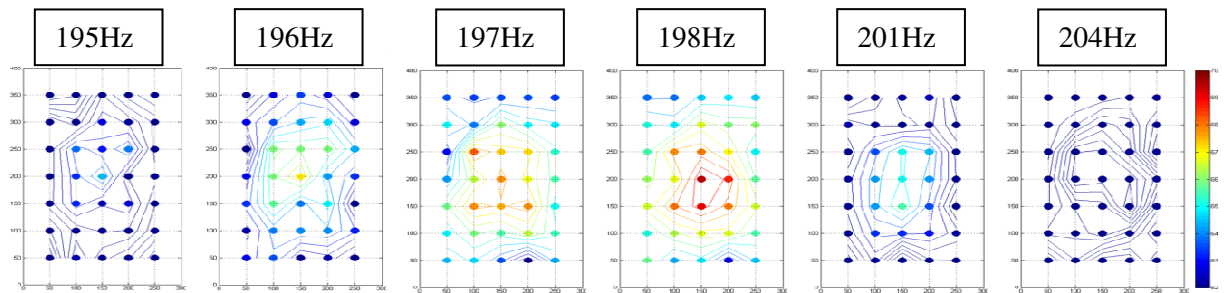
The radiating surface (and the corresponding acquisition area) is discretised in 12 sub-surfaces. The radiated sound power is then calculated as

$$P = \sum_{i=1}^{12} I_i S_i , \quad (3)$$

where I_i is the measured normal intensity at the corresponding central point of sub-surface “i” with surface S_i . The intensity is measured twice, respectively, with and without the closing plate set on the top of the cavity. Figures 5 and 6 show the acoustic radiated power (expressed in dB, when the reference power level is equal to 10^{-12} W) for both open and closed cavity measurements, and the resulting IL, for the aluminium plate and the sandwich panel, respectively. For the sake of clarity, here only results up to 700Hz are shown. Later on the full studied frequency region will be plotted.



The position of dips and peaks in the resulting IL correspond to the natural frequencies of the coupled system, “test-panel + acoustic cavity”. These modes can be either structurally or acoustically dominated, depending on the specific characteristics of the two sub-systems. The first drop in the IL corresponds in both cases to the first bending mode of the panel (high radiation efficiency), which occurs around 200Hz for the clamped aluminium plate and around 100Hz for the simply supported sandwich panel. With intensity measurements it is also possible to map the acoustic power distribution over the acquisition grid. For the aluminium plate this is illustrated in Figure 7, looking at the distribution around the peak at 200Hz. In this case a denser acquisition mesh (35points) is used. The pattern of the first bending mode is clearly visible.



In order to understand and discuss the locations of the remaining drops and peaks the coupled behaviour must be studied and therefore, a coupled numerical model is developed and proposed in the following sections.

3 Numerical study of IL

A numerical model of the described set-up allows the analysis of the coupled system and moreover, once updated and validated, allows to carry out various analyses (i.e., sensitivity analyses with respect to the unit cell geometrical or material properties and so on) with no need for additional time consuming and expensive experimental tests. In this section details about the acoustic numerical model of the cavity and the structural FE model of the tested panels are presented, followed by the coupled system composition. At the end of this part some first IL numerical evaluations are shown. MD/Nastran 2010 R3b and LMS.Virtual Lab Rev8b are used for performing the numerical simulations.

3.1 Acoustic cavity model

An acoustic BE model of the rigid acoustic cavity is developed and shown in Figure 8 (left side). In the first stage the full sand-box is modelled and reflections of sound waves at the concrete floor of the semi-anechoic room are also taken into account by including a reflecting plane 7cm below the box, as shown in the same picture. Numerical analyses indicate the negligible effects of both the lower box (hosting the loudspeaker) and the floor reflections on the acoustic cavity behaviour and final pressure field.

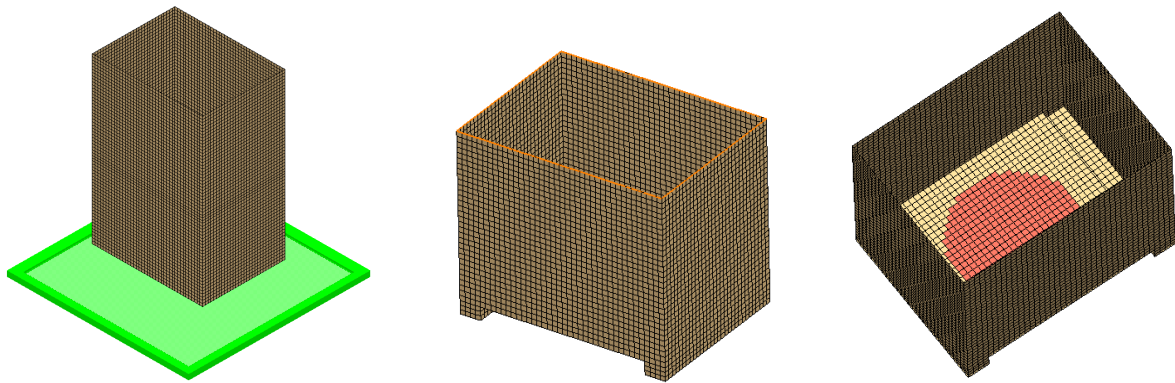


Figure 8: Acoustic cavity modelling – from left to right: initial full model –final simplified model –final simplified model with loudspeaker elements

Therefore, this model has been simplified as shown in Figure 8 (centre and right side). Now it only simulates the upper cavity of the experimental sand-box.

An FE model is first used to evaluate the uncoupled natural frequencies for this upper cavity (considered completely enclosed by rigid walls). Acoustic mode shapes up to 1000Hz are shown in Table 4. The same model is used later on to evaluate the coupled system's modal behaviour.

Once the final BE model is defined, it has to be prepared for the forced response analysis (Indirect Boundary Element Analysis, I-BE). A subset of elements (partially visible in Figure 8, right side) is identified to simulate the vibrating membrane of the loudspeaker. The latter is modelled as a constant panel velocity boundary condition. A constant amplitude (1m/s) normal velocity vector (directed into the cavity) is applied on those elements. Another set of BCs is defined when the open cavity case is analysed. It represents the zero jump of pressure at the top edge nodes (open edges on the top of the cavity in Figure 8, centre).

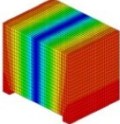
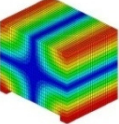
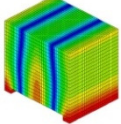
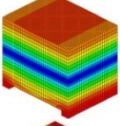
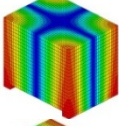
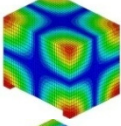
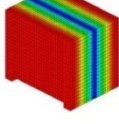
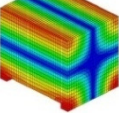
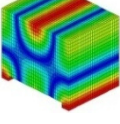
Mode number	Mode shape	f [Hz]	Mode number	Mode shape	f [Hz]	Mode number	Mode shape	f [Hz]
1		419	4		665	7		835
2		531	5		705	8		874
3		567	6		777	9		973

Table 4: Uncoupled acoustic modes for the upper box cavity

3.2 Specimen FE model

An FE model is created to simulate the natural behaviour and vibro-acoustic response of the tested specimens. For the aluminium plate this results in a quite simple model, with 1496 nodes and 1419 shell (CQUAD4) elements and clamped on its edges. In the case of the examined sandwich panel a detailed description of the unit cell (Figure 9, left side) has to be provided. Duplication of this unit cell along the two in-plane axes leads to a final model (Figure 9, right side) which consists of 129214 nodes and 198810 elements (4- and 3-nodes shell elements), considered simply supported on its edges.

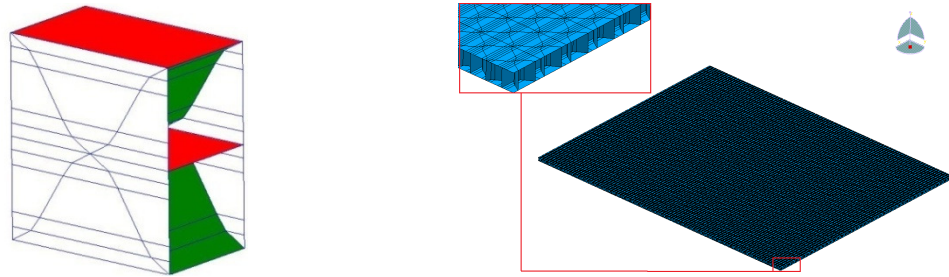


Figure 9: On the left detail of a unit cell – On the right FE model of the TorHex core sandwich panel

Experimental validation of the structural model of the panel is based on an EMA carried out up to 300Hz on the TorHex panel freely suspended. The good agreement found between the experimental and numerical results is shown in Table 5 (NB. 4th and 8th numerical modes are missing in the experimental results), in terms of natural frequencies and Modal Assurance Criterion (MAC, used to compare corresponding eigenvectors). The first ten uncoupled structural modes for the simply supported case (approximated by fixing the translational degrees of freedom of all the nodes at the lower skin edges) are listed in Table 6.

Mode pair	Num.Mode No.	f [Hz]	Exp.Mode No.	f [Hz]	MAC [%]
1	1	49	1	49	83
2	2	57	2	59	88
3	3	105	3	108	74
4	5	140	4	135	90
5	6	163	5	164	75
6	7	215	6	211	77
7	9	286	7	279	64

Table 5: Correlation results between EMA and FEM analysis on the TorHex panel freely suspended

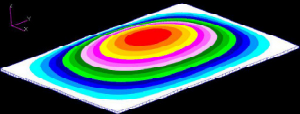
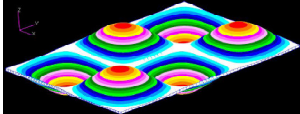
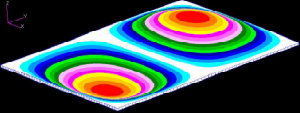
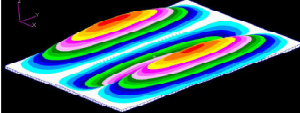
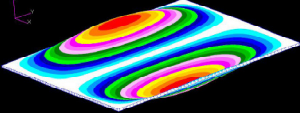
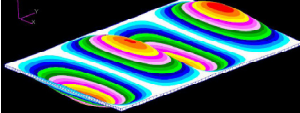
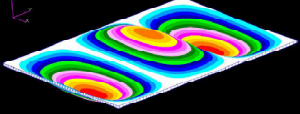
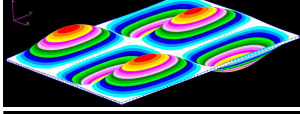
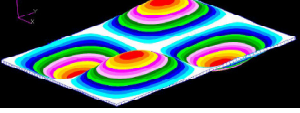
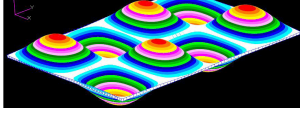
Mode	Mode shape	f [Hz]	Mode	Mode shape	f [Hz]
1		91	6		441
2		166	7		456
3		218	8		475
4		298	9		535
5		307	10		620

Table 6: Numerical modal analysis results for the simply supported TorHex panel

3.3 Coupled system

The numerical simulation has to provide the radiated sound power for both the open and closed cases. This requires two models: one boundary element model for the open box (as described in 3.1) and one for the closed box. In the latter case the structural FE model built for the test panel has to be coupled to the BE model developed for the acoustic cavity. In order to get a final model size that requires a reasonable computational effort (especially for the sandwich plate model), the structural modes of the panel are projected on a coarser mesh. For the TorHex panel the maximum number of wavelengths found numerically up to 2000Hz is 4 in the longitudinal direction (mode at 1991Hz) and 3 in the width (mode at 1995Hz). The use of 10 elements per bending wavelength (rule of thumb) leads to a coarser mesh of 30x40 elements on which the structural modes are projected. In Figure 10 the coupled system with the coarser mesh (closing the acoustic cavity from the top) is shown. Of course this coarser mesh is not present for the simulation on the open box (where zero jump of pressure BCs are applied instead at the top edges).

In order to determine the sound power from the calculated potentials a set of field points is defined. It consists of a plane located at 25cm and 5cm above the specimen for the aluminium and TorHex panel respectively, to better simulate the real measurement set-up.

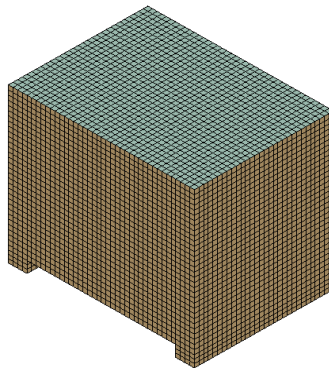


Figure 10: Acoustic cavity and testing panel on the top - BE models

From I-BE simulation the radiated power is calculated and the results are shown in Figures 11 and 12, compared with the experimental values for the aluminium plate and the TorHex panel up to 1250Hz, respectively. The numerical frequency resolution is 10Hz.

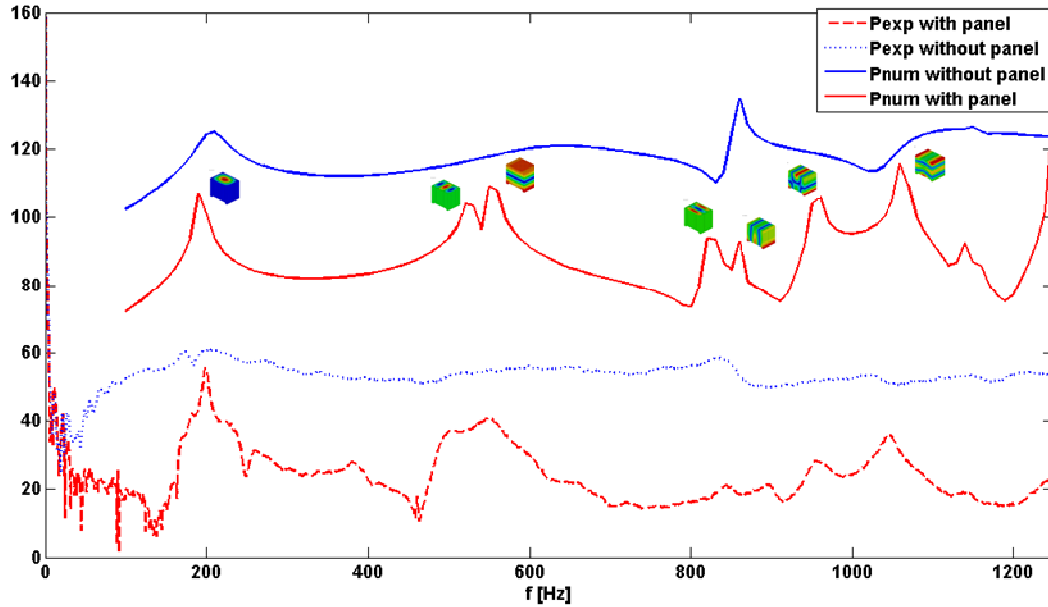


Figure 11: Experimental and numerical radiated power [dBW], open and closed box – Aluminium

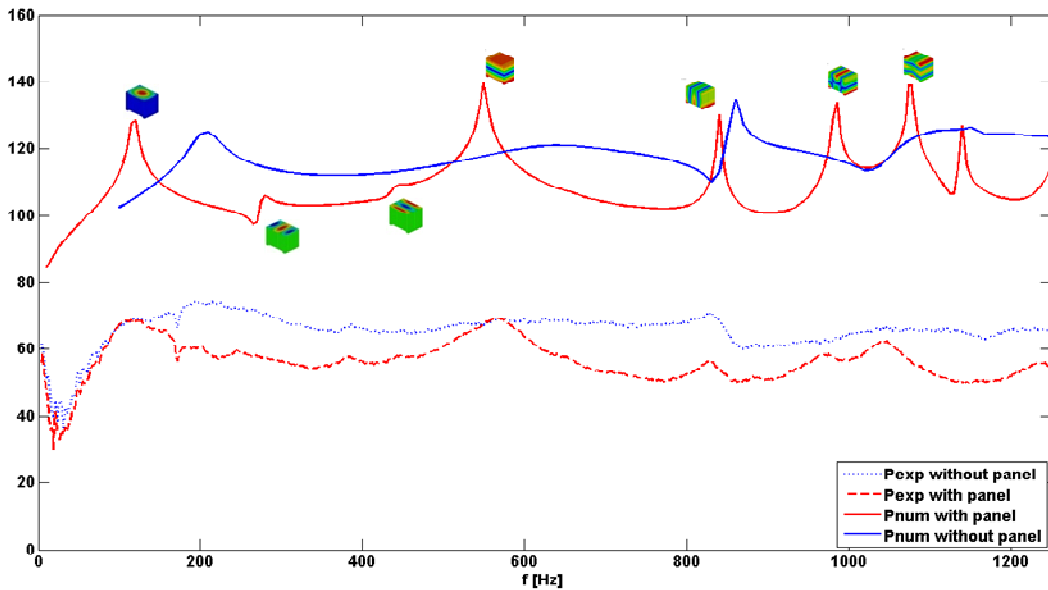


Figure 12: Experimental and numerical radiated power [dBW], open and closed box – TorHex

A nice agreement is found between numerical and experimental trends for both examined cases. Few remarkable comments can be already made. There is no structural nor acoustic damping of any kind in these first numerical models. Further updates will follow in the next steps. The absolute power levels are not relevant for the IL calculation (it just depends on their difference). The vertical shift between the experimentally recorded power levels and the simulations is due to the excitation amplitude (imposed to be 1m/s constant amplitude in the numerical model, it does not represent the real acting value). In the frequency region around [100-200] Hz the experimental radiated power curve seems to be flatter as highlighted in the zoom of Figure 13 by the black dashed lines (left side-aluminium plate, right side-

TorHex panel). This trend does not appear in any numerical simulation and is most likely due to the semi-anechoic room in which the set-up is located (which has a cut-off frequency of around 300Hz and is not included in the numerical model).

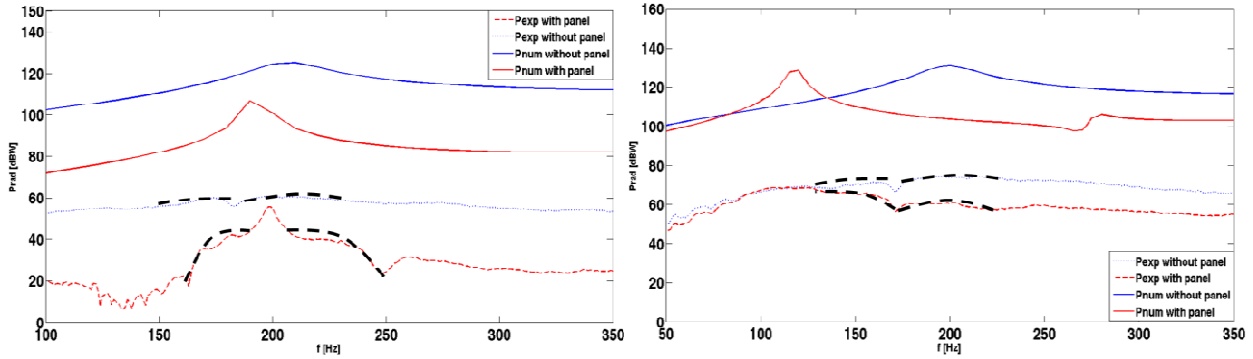


Figure 13: Experimental and numerical radiated power [dBW], open and closed box Aluminium (left) and TorHex (right)

The coupled system analyses show from a panel point of view how only the structurally dominating modes with an uneven number of half wavelengths have a relevant effect on the acoustic transmission. At these modes a peak in the radiated power for the closed cavity case is apparent (as reported in Figures 11 and 12, where the corresponding acoustic parts of the coupled mode shapes are shown). In the examined frequency window the 1-1, 1-3 and 3-1 bending modes can be observed. The other structural modes with an even number of bending half wavelength in the length and/or width direction are such that for each air particle forced to move by the panel's deflection there is another neighbouring particle that undergoes an opposite movement (acoustic short-circuit effect). This tends to cancel out the pressure radiation, especially in the far field. Some acoustic cavity modes also appear to be efficient couplers. In particular, the second acoustic mode (around 550Hz, well visible in both cases) is quite effective on the global radiation, since it is due to the vertical standing wave in the acoustic cavity.

3.4 Numerical IL

Figure 14 shows the comparison between the experimental and numerical IL for the aluminium and TorHex panel (left and right side respectively).

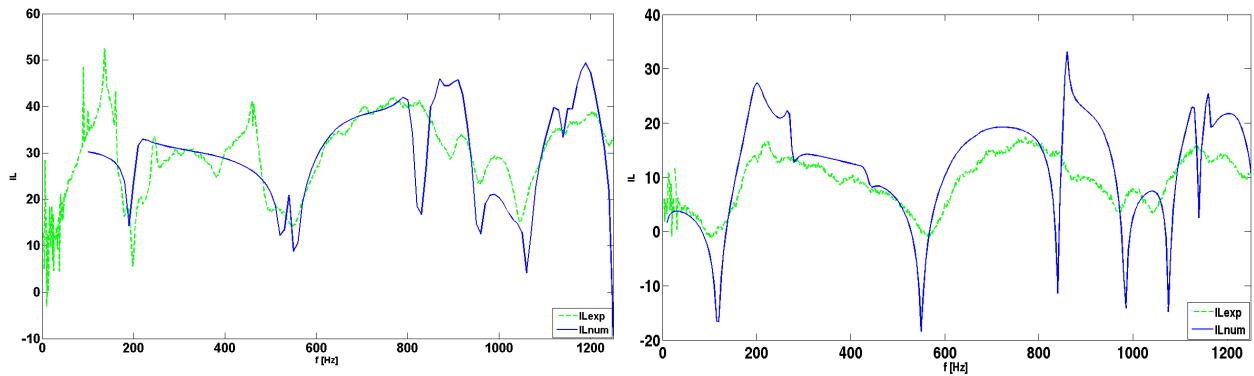


Figure 14: Experimental and numerical IL. Left side: aluminium plate. Right side: TorHex panel

The difference between simulated and experimental IL can be efficiently reduced when the numerical model is updated. As shown in the next paragraph, updating the structural damping of the studied panel and the acoustic impedance of the cavity walls yields an accurate tool for IL prediction.

4 Updated numerical model

The updating procedure mainly focuses on modal damping and acoustic impedance updating. These are the two main parameters not known at the beginning when the models were defined. Modifications of these two quantities allow taking advantage of their separate actions. Modal damping acts in fact mainly on those peaks representing coupled resonances which are structurally dominated. On the other hand acoustic damping, applied in the form of real normal impedance on the inner sand-box's walls, influences those peaks driven by cavity modes. It has to be remarked that while the modal damping depends on the specific coupled system (in particular, applied BCs and examined panel) the acoustic damping can be considered to be a property of the acoustic cavity and then a unique value can be used to analyse different cases.

4.1 Optimized η and Z_{ac}

Figure 14 shows a good correlation for the aluminium plate up to 800Hz. For the sandwich panel on the other hand, important mismatches with the experimental results occur already at the first resonances. This is most likely due to the unknown inaccuracy in the BCs simulation. The TorHex panel is simply supported on its edges and plasticine is used to seal them all around. This introduces an important damping contribution into the system (completely discarded in the first model). The plasticine also adds some stiffness, that is definitely higher than the zero bending stiffness model of the pinned boundary conditions.

The real valued acoustic impedance is varied in a very wide range, [10-100-3000-6000-12000-20000-100000] kg/m²/s. The modal damping is also modified in order to reduce the difference between the numerical and experimental IL. The objective function to be minimised expresses the difference between the averaged experimental IL and the averaged numerical IL. While for the structural damping two different values are found for these two panels (1% modal damping for the clamped aluminium plate and 7% for the TorHex sandwich panel, treated with plasticine all around its edges), the same updated acoustic impedance value (20000 kg/m²/s real acoustic impedance on the inner cavity walls) is applied in both cases to the cavity.

4.2 Updated numerical IL

Figures 16 and 17 show the final comparison between experimental and optimized numerical IL (narrow and third octave frequency bands). The updated settings, developed on the aluminium plate case, show very nice results. The predicted IL matches almost perfectly with the experimental values for this system. The same procedure applied to the sandwich panel also shows good results. In Figure 17 the higher difference in terms of IL in the lower frequency region (up to 800Hz) is especially due to the relatively poor numerical resolution (10Hz) compared to the frequency bands' width (third octave bands tend to be wider going up in frequency). This is confirmed by the good agreement between experimental and numerical results in the same region in Figure 16. Around some frequency values (as 800Hz and 1200Hz in this specific window) the predicted IL takes the distance from the experimental results and then starts to follow it again. This narrow band difference (well visible in Figure 16) does not influence particularly the comparison between the averaged values (Figure 17) and comes from some mismatches in the radiated power simulations as shown in Figure 15 (where the dotted curves on the bottom are the experimental data, while the dash-dot on the top come from the first numerical model and the full lines from the last updated simulation). Comparing the average IL levels for these panels, it is easy to see how the sandwich structure exhibits worse reduction performance (overall lower IL). The weight of the light structure is much lower than the correspondent value of the aluminium panel ($w_{TorHex} \sim 160g$ vs. $w_{Al} = 1.27kg$). This essentially improves the sound reduction abilities of the latter. According to the conclusions reported in [9], this feature could be improved coupling the same core structure to a skin layer of stiffer material. In this case satisfactory performance can be achieved still preserving a certain weight saving [9].

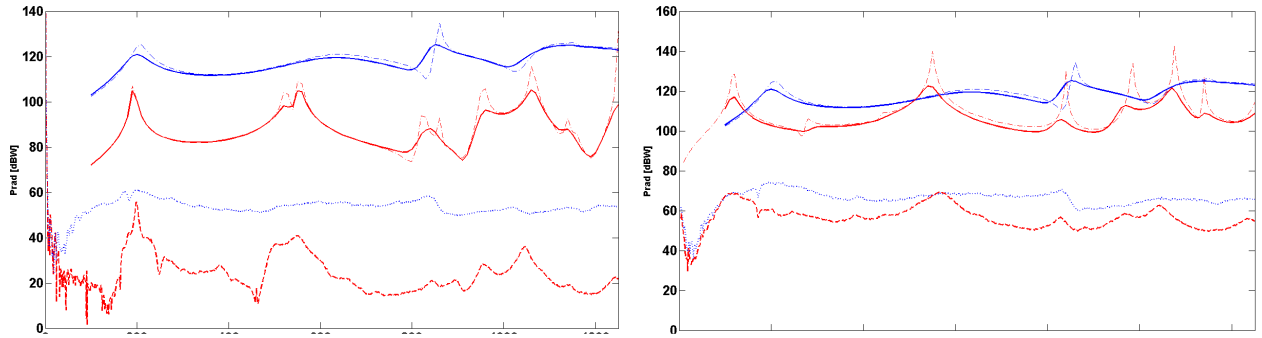


Figure 15: Radiated power comparison: Aluminium plate (left) - TorHex panel (right)

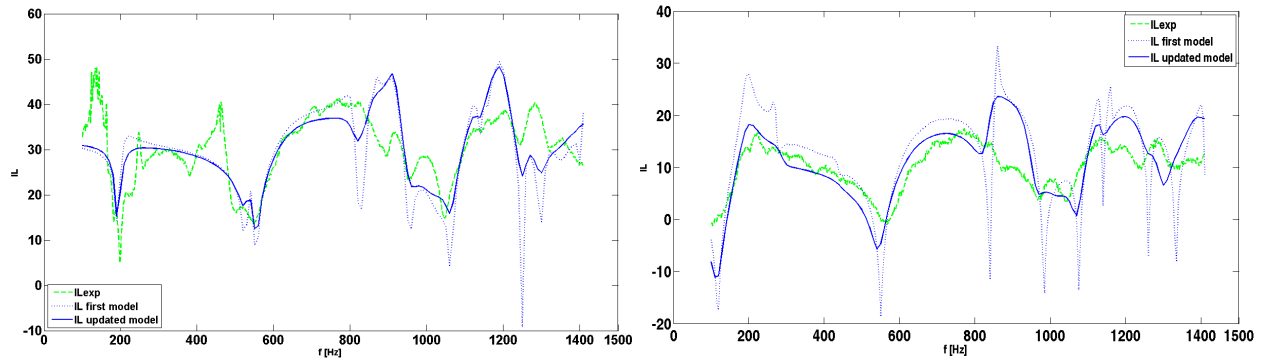


Figure 16: IL comparison narrow band: Aluminium plate (left) - TorHex panel (right)

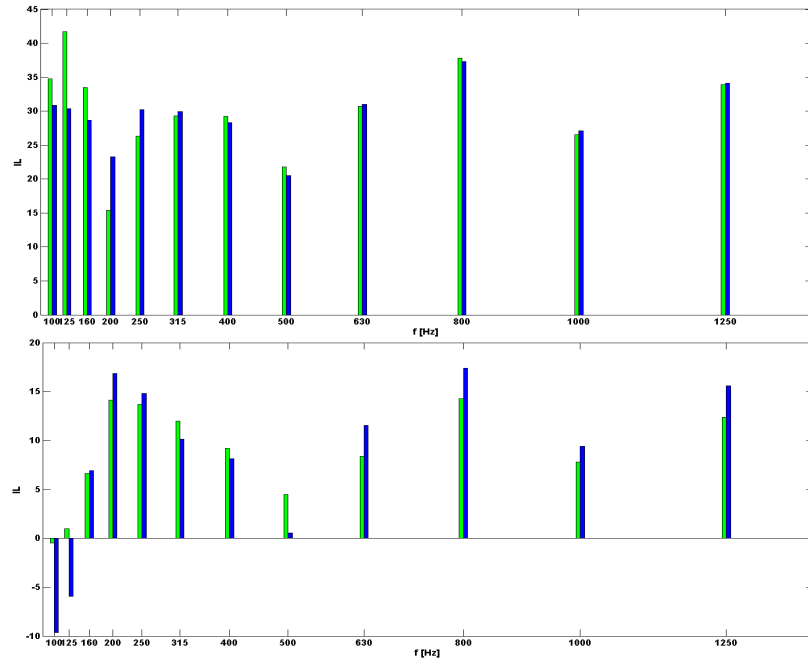


Figure 17: IL comparison third octave bands: Aluminium plate (top) - TorHex panel (bottom)

5 Conclusions

A numerical model is first developed and then updated in order to predict the IL of flat panels. The updating procedure is based on the comparison of experimental results with predictions obtained by the

numerical model for 2 different panels, an aluminium and a sandwich panel. These results encourage the authors to further investigate and validate the reliability of the numerical models. Based on the same models some sensitivity analyses are already on-going to study the vibro-acoustic properties of a new and “improved” TorHex core sandwich structures. Furthermore, a new test facility is being set up to allow multiple excitation sources (mechanical and acoustic) on specimens of various thickness and size.

Using the existing and the new test set-up the goal is to engineer lightweight sandwich material core structures to exhibit optimal desired vibro-acoustic properties.

Acknowledgements

The Fund for Scientific Research - Flanders (F.W.O.), Belgium, is gratefully acknowledged for its research support. Furthermore, the authors also kindly acknowledge the European Commission for their support of the Marie Curie EST Project SIMVIA2 (<http://www.simvia2.eu>, contract nr. MEST-CT-2005-020263), from which the first author holds a Research Training grant.

References

- [1] C. D. Johnson, N.R. Bauld Jr., *Dynamic Stability of Rectangular Sandwich Plates under Pulsating Loads*, Clemson University, Clemson, S.C. (1968).
- [2] N.S. Khot, V.B. Venkayya, C.D. Johnson, V.A. Tischler, *Optimum design of advanced composite structures for static loads*, Air Force Flight Dynamics Laboratory, Wright-Patterson Air Force Base, Ohio (1972).
- [3] Y. Frostig, O.T. Thomsen , *On the free vibration of sandwich panels with a transversely flexible and temperature-dependent core material – Part I: Mathematical formulation*, Composites Sciences and Technology, Vol. 69, (2009), pp. 856-862.
- [4] C. D. Johnson, N.R. Bauld Jr., *Transmission Loss optimization in acoustic sandwich panels*, College of Engineering, University of Massachusetts, Amherst, Massachusetts (1986).
- [5] T. Wang, S. Li, Steven R. Nutt, *Optimal design of acoustical sandwich panels with a genetic algorithm*, Applied Acoustics, Vol. 70, (2009), pp. 416-425.
- [6] C.-M. Lee, Y. Xu, *A modified transfer matrix method for prediction of transmission loss of multilayer acoustic materials*, Journal of Sound and Vibration, Vol. 326, (2009), pp. 290-301.
- [7] S. Adali, A. Richter , V. E. Verijenko, *Non-probabilistic modeling and design of sandwich plates subject to uncertain loads and initial deflections*, Int. J. Engng Sci., Vol. 33, No.6, (1995), pp. 855-866.
- [8] A. Baz, *Active control of periodic structures*, J. Vib. Acoust., Vol.123, (2001) pp. 472-480.
- [9] M. Vivolo, B. Pluymers, D. Vandepitte, W. Desmet, *Vibro-acoustic characteristics of TorHex honeycomb sandwich panels*, *Proceedings of The TRA Transport Research Arena Europe2010*, Brussels, Belgium, 2010, June 7-10, pp. 233.
- [10] M. Vivolo, B. Pluymers, D. Vandepitte, W. Desmet, *Numerical evaluation of the Insertion Loss of lightweight TorHex sandwich panels*, *Proceedings of The Tenth International Conference on Recent Advances in Structural Dynamics*, Southampton, UK, 2010, July 12-14
- [11] J.Pflug I.Verpoest and D.Vandepitte, *Folded honeycomb cardboard and core material for structural applications*, *Proceedings of the 5th Sandwich Construction conference*, 2000, Zurich
- [12] J.Pflug and F.Xinyu, *Development of sandwich material with polypropylene/natural fibre skins and paper honeycomb core*, *Proceedings of 10th European Conference on Composite Materials (ECCM-10)*, Belgium, 2002, paper 331
- [13] J. Pflug, I. Verpoes, *Folded-sheet honeycomb structure (Faltwabe)*, *patent application PCT/EP96/03121*, granted as European patent EP0839088 (Nov. 1999) and as American patent US6183836, 2001
- [14] W. Desmet, B. Pluymers, P. Sas, *Vibro-acoustic analysis procedures for the evaluation of the sound insulation characteristics of agricultural machinery cabins*. *Journal of Sound and Vibration*, Vol.266, (2003), pp.407-441
- [15] V.L. Metcalf, W. Ferdinand, *Noise Transmission Characteristics of Aircraft-Type Composite Panels* , NASA Langley Research Canter, Hampton, VA - 19
- [16] G.A. Baum, D.C. Brennan, C.C. Habeger, *Orthotropic elastic constants of paper*, Tappi Journal, Vol. 64, (1981), pp. 97-101
- [17] K.K. Ang, *The core-kin bond strength of sandwich panels with paper honeycombs and thermoplastic honeycombs*, Master thesis, Faculty of Applied Sciences, Dep. MTM, K.U.L, 2003-2004